Molecular Neurobiology (2019) 56:6095–6105
https://doi.org/10.1007/s12035-019-1471-z

Rab18 Collaborates with Rab7 to Modulate Lysosomal and Autophagy Activities in the Nervous System: an Overlapping Mechanism for Warburg Micro Syndrome and Charcot-Marie-Tooth Neuropathy Type 2B

Fang-Shin Nian[1,2] · Lei-Li Li[1] · Chih-Ya Cheng[3] · Pei-Chun Wu[4,5] · You-Tai Lin[4] · Cheng-Yung Tang[4] · Bo-Shiun Ren[1] · Chin-Yin Tai[6] · Ming-Ji Fann[4,5] · Lung-Sen Kao[4,5] · Chen-Jee Hong[5,7,8] · Jin-Wu Tsai[1,5,9]

Received: 28 November 2017 / Accepted: 10 January 2019 / Published online: 5 February 2019

Abstract

Mutations in *RAB18*, a member of small G protein, cause Warburg micro syndrome (WARBM), whose clinical features include vision impairment, postnatal microcephaly, and lower limb spasticity. Previously, our *Rab18*$^{-/-}$ mice exhibited hind limb weakness and spasticity as well as signs of axonal degeneration in the spinal cord and lumbar spinal nerves. However, the cellular and molecular function of RAB18 and its roles in the pathogenesis of WARBM are still not fully understood. Using immunofluorescence staining and expression of Rab18 and organelle markers, we find that Rab18 associates with lysosomes and actively traffics along neurites in cultured neurons. Interestingly, *Rab18*$^{-/-}$ neurons exhibit impaired lysosomal transport. Using autophagosome marker LC3-II, we show that Rab18 dysfunction leads to aberrant autophagy activities in neurons. Electron microscopy further reveals accumulation of lipofuscin-like granules in the dorsal root ganglion of *Rab18*$^{-/-}$ mice. Surprisingly, Rab18 colocalizes, cofractionates, and coprecipitates with the lysosomal regulator Rab7, mutations of which cause Charcot-Marie-Tooth (CMT) neuropathy type 2B. Moreover, Rab7 is upregulated in Rab18-deficient neurons, suggesting a compensatory effect. Together, our results suggest that the functions of RAB18 and RAB7 in lysosomal and autophagic activities may constitute an overlapping mechanism underlying WARBM and CMT pathogenesis in the nervous system.

Keywords *Rab18* · Warburg micro syndrome · Neuron · Axonal degeneration · Vesicle trafficking · Lysosome · Charcot-Marie-Tooth · *Rab7* · Autophagy · LC3

Electronic supplementary material The online version of this article (https://doi.org/10.1007/s12035-019-1471-z) contains supplementary material, which is available to authorized users.

✉ Jin-Wu Tsai
tsaijw@ym.edu.tw

[1] Institute of Brain Science, National Yang-Ming University, Taipei, Taiwan

[2] Program in Molecular Medicine, National Yang-Ming University and Academia Sinica, Taipei, Taiwan

[3] Department of Pediatrics, Taipei Veterans General Hospital, Taipei, Taiwan

[4] Department of Life Sciences and Institute of Genome Sciences, National Yang-Ming University, Taipei, Taiwan

[5] Brain Research Center, National Yang-Ming University, Taipei, Taiwan

[6] Institute of Molecular Biology, Academia Sinica, Nankang, Taipei, Taiwan

[7] Division of Psychiatry, School of Medicine, National Yang-Ming University, Taipei, Taiwan

[8] Department of Psychiatry, Taipei Veterans General Hospital, Taipei, Taiwan

[9] Biopotonics and Molecular Imaging Research Center, National Yang-Ming University, Taipei, Taiwan

Introduction

Warburg micro syndrome (WARBM) is an autosomal recessive developmental and degenerative disorder characterized by abnormalities in the brain, eye, and reproductive system [1–3]. Neurological phenotypes include postnatal microcephaly, mental retardation, truncal hypotonia, epilepsy, and progressive limb spasticity. Magnetic resonant imaging (MRI) studies further showed structural abnormalities in the central nervous system, including bilateral polymicrogyria, hypogenesis of the corpus callosum, and cerebellar vermis hypoplasia [2–5]. To date, mutations in four genes have been found to cause this devastating disorder: *Rab3GAP1*, *Rab3GAP2*, *Rab18*, and *TBC1D20* [6–9], all of which are related to Rab proteins.

Rab proteins are small GTPases belonging to the Ras superfamily and regulate vesicle transport processes in different cell types. They recruit a number of effector proteins to assist multiple steps of membrane trafficking, including budding, uncoating, transport, tethering, and fusion [10]. Besides WARBM, mutations in other *RAB* genes have been identified to cause various neurological diseases, such as Charcot-Marie-Tooth type 2B neuropathy (*RAB7*) [11, 12], Carpenter syndrome (*RAB23*) [13–15], Griscelli syndrome (*RAB27A*) [16–19], and X-linked mental retardation (*RAB39B*) [10, 20, 21].

Rab18 is widely expressed in most animal tissues [22, 23] but exhibits distinct subcellular localizations and biological functions in different cell types. For example, Rab18 was found at lipid droplets in the adipocytes, fibroblasts, hepatocytes, and epithelial cells and was involved in lipogenesis and lipolysis [24–32]. RAB18 was also critical for maintaining normal ER structure and ER-Golgi trafficking, possibly regulated by RAB3GAP1, GAB3GAP2, and TBC1D20, in various non-neuronal cells [33–36]. In the endocrine, neuroendocrine, and pituitary melanotropic cells, Rab18 was localized at the secretory granules, suggesting that Rab18 may be important for the regulation of secretory activities [37, 38]. Rab18 has also been implicated in targeting viral particles and bacteria to various cellular structures [39–43]. Lastly, RAB18 was also found to modulate macroautophagy and proteostasis in human fibroblasts in RAB3GAP1- and RAB3GAP2-dependent manners [44], implicating a potential involvement of autophagy in WARBM. However, most of these studies were conducted in non-neuronal cells, and therefore, the neuronal roles of RAB18 in WARBM remain largely unexplored.

To date, two *Rab18* knockout mouse models generated by gene targeting ($Rab18^{Gt(EUCE0233a03)Hmgu}$) or ENU-mutagenesis ($Rab18^{-/-(ENU)}$) have been used to investigate its role in the pathogenesis of WARBM [45, 46]. Both mouse lines exhibited hind limb weakness and clasping/clenching when hung by the tail. In addition, $Rab18^{Gt(EUCE0233a03)Hmgu}$ mice also showed congenital nuclear cataracts and atonic pupils [45] whereas $Rab18^{-/-(ENU)}$ mice exhibited microphthalmia, microgenitalia, and hypoplastic corpus callosum [46]. All these phenotypes recapitulated clinical representations found in WARBM patients. However, the cellular functions of RAB18 in neurons and their roles in causing neural phenotypes in WARBM require further investigation.

In the current study, we use neuronal culture and *Rab18* knockout mouse models to investigate cellular and molecular functions of Rab18 in the nervous system. We find that Rab18 associates with lysosomes and facilitates lysosomal trafficking and autophagy in neurons. Deficiency of Rab18 results in defects in lysosomal transport and aberrant autophagy activities, which may cause axonal degeneration and contribute to the symptoms in the nervous system observed in patients with WARBM. Surprisingly, we also find that Rab18 and Rab7 interact on the lysosome and may compensate each other genetically, implicating that WARBM and CMT neuropathy may share overlapping mechanisms in their pathogenesis.

Materials and Methods

Cell Culture and Transient Transfection

PC12 and HEK293T cells (ATCC) were cultured in DMEM/10% horse serum/5% fetal bovine serum/penicillin streptomycin and DMEM/10% fetal bovine serum/penicillin streptomycin (Invitrogen), respectively. All cells were plated on 12-mm-diameter glass coverslips or glass-bottomed dishes coated with poly-D-lysine (Sigma-Aldrich) and maintained at 37 °C in a humidified atmosphere with 5% CO_2 until use. PC12 cells were differentiated into neuronal-like cells by incubating with 100 ng/ml nerve growth factor (NGF, Sigma-Aldrich) for at least 3 days. Transient transfection was performed using Lipofectamine® 3000 or LTX according to the manufacturer's instructions (Invitrogen).

Primary Cortical Neuron Culture and Lentivirus Transduction

Cortical neurons were prepared from E18.5 Sprague-Dawley rats or E16.5–18.5 embryos of $Rab18^{+/+}$, $Rab18^{+/-}$, and $Rab18^{-/-}$ mice via papain-mediated dissociation (Sigma-Aldrich) according to our previous report [47, 48]. Neurons were cultured in NeuralQ Basal Medium/L-glutamine/2% GS21/penicillin/streptomycin (MTI-GlobalStem). Lentivirus carrying Rab18 shRNA or scramble sequence was transduced into primary cortical neurons at DIV 3–4. Two of Rab18 shRNA used in this study were TRCN0000021981 (CGTGAAGTCGATAGAAATGAA) and TRCN0000177028 (GATGGAAATAAGGCTAAACTT). Scramble sequence (CCTAAGGTTAAGTCGCCCTCG) was used as negative control. All shRNA reagents and

lentivirus particles were purchased from the National RNAi Core Facility at Academia Sinica, Taiwan.

Western Blot Analysis

Total cell lysates from cultured PC12 cells or cortical neurons were obtained by lysing cells in RIPA buffer (50 mM of Tris-HCl pH 8.0, 150 mM of NaCl, 1% NP-40, 0.5% of sodium deoxycholate, and 0.1% of SDS) supplemented with protease inhibitor cocktail (Thermo Scientific) and phosphatase inhibitor (Roche). Protein concentrations were determined with BCA protein assay (Thermo Scientific). Western blotting was performed with primary antibodies: rabbit anti-Rab18 (Proteintech Group; diluted 1:100), mouse anti-Rab18 (Proteintech Group; diluted 1:1000), mouse anti-GAPDH (GeneTex; diluted 1:5000), and mouse anti-α-tubulin (Proteintech Group; diluted 1:5000). GAPDH and α-tubulin were used as loading controls. The primary antibodies were detected with horseradish peroxidase (HRP)-conjugated secondary antibodies: anti-mouse (GeneTex; diluted 1:10,000) and anti-rabbit (Sigma-Aldrich; diluted 1:10,000). The signals were developed with ECL reagent (Millipore) and detected by Luminescence/Fluorescence Imaging System LAS-4000 (Fujifilm). The quantification of protein band intensities was analyzed by ImageJ (NIH) software. To investigate the roles of Rab18 in the lysosomal functions and autophagy, Rab7 and LC3-II expression in Rab18 knockdown or knockout neurons was determined by Western blotting as described. Rab7 antibody (Abcam; diluted 1:500) and LC3 antibody (Proteintech Group; diluted 1:3000) were used; α-tubulin (Proteintech Group; diluted 1:5000) was used as a loading control.

Live Cell Imaging and Analysis

For live cell imaging, cells were plated on 35-mm-diameter glass-bottomed dishes. EGFP and mRFP-tagged proteins were visualized 24 h after transfection. Time-lapse images were acquired sequentially every second or every 2 s for 2 min at 37 °C by a fluorescent microscope (AxioObserver, Carl Zeiss) with 100× oil immersion objective (1.4 NA) [49, 50]. To determine the velocity of lysosome transport in primary cortical neurons cultured from *Rab18*$^{+/+}$ and *Rab18*$^{-/-}$ mice, the rate of lysosomes was analyzed by Retrac software (version 2.1.01). Single particle tracking was performed by TrackMate, an open-source ImageJ, and Fuji plugin for automated or manual tracking of single particles.

Immunocytochemistry

Cells were fixed by 4% paraformaldehyde for 20 min at RT and permeabilized by Triton X-100 for 30 min at RT. Detection of Rab18 was performed using rabbit anti-Rab18 (Proteintech Group; diluted 1:50) and Alexa Fluor® 488 or 594 goat anti-rabbit antibodies (Invitrogen, 1:400). The coverslips were mounted onto the glass slides with VECTASHIELD® Mounting Media.

Organelle Labeling

EGFP-Sec61β, EGFP-Rab5, and EGFP-Rab3A were used as markers of ER, early, and late endosomes, respectively. These plasmids were transfected into NGF-differentiated PC12 cells for 48 h. For mitochondria labeling, 500 nM of MitoTracker® probe (Invitrogen) was used to treat cells for 30 min at 37 °C. Cells were fixed and then immunostained with the Rab18 antibody as described in the "Immunocytochemistry" section. For lysosome labeling, cells were treated with 50 nM of LysoTracker® probe (Invitrogen) for at least 15 min at 37 °C and observed using live cell imaging.

Confocal Microscopy

The coverslips were imaged with a Zeiss LSM 700 laser scanning confocal microscope using a 100× oil immersion objective (1.4 NA). The excitation/emission wavelengths were 488/507 nm (EGFP), 554/576 nm (MitoTracker® probe), 590/617 nm (Alexa Fluor® 594), and 350/470 nm (DAPI). *Z*-series images were collected at 1-μm intervals. Maximum intensity projections were performed by the ZEN software (Carl Zeiss). Colocalization analysis was performed using Colocalization Threshold plugin in FIJI/ImageJ software (NIH) [51].

Immunoprecipitation

HEK293T cells were plated on 10-cm culture dishes and cotransfected with EGFP-Rab18 or EGFP control together with mRFP-Rab7. Twenty-four hours after transfection, the cells were lysed in 0.1% Triton X-100 and 0.1% SDS supplemented with protease inhibitor cocktail (Sigma-Aldrich) on ice for 30 min and then centrifuged in a tabletop centrifuge (Eppendorf) at full speed for 30 min to obtain lysate. Equal amount of lysate was incubated with GFP-Trap® beads according to the manufacturer's instructions (ChromoTek) to isolate EGFP interacting proteins. Western blotting was performed with primary antibodies: mouse anti-Rab7 (Abcam; diluted 1:1000) and mouse anti-GFP (Invitrogen; diluted 1:1000). The primary antibodies were detected with horseradish peroxidase (HRP)-conjugated secondary antibodies: anti-mouse (GeneTex; diluted 1:10,000).

Lysosome Purification

Lysosomal fractions were isolated from adult mouse brain lysates by density gradient centrifugation according to the manufacturer's protocol (Sigma-Aldrich; LYSISO1). Briefly,

mouse brain tissues were homogenized with sonication. Differential centrifugation (1000×*g* for 10 min and 20,000×*g* for 20 min) was then used to obtain a crude lysosomal fraction (CLF), which still contained a mixture of light mitochondria, lysosomes, peroxisomes, and ER. The CLF was then diluted with 19% OptiPrep Density Gradient Medium Solution, followed by gradient centrifugation (150,000×*g* for 4 h). Further purification of the lysosomes was achieved by addition of $CaCl_2$ to a final concentration of 8 mM, followed by low-speed centrifugation (5000×*g* for 15 min) to precipitate the rough ER and mitochondria.

Electron Microscopy

Electron microscopy was performed as previously described [46]. Briefly, the spinal cord was dissected immersed in 2.5% glutaraldehyde in 0.1 M PB (pH 7.4) overnight. After washing in the same buffer, the tissue was then post-fixed in 1% OsO_4 for 2 h, dehydrated in a graded series of ethanol, infiltrated with propylene oxide/Spurr's resin, and polymerized at 70 °C for 8 h. Ultrathin sections (60–70 nm thick), prepared with an ultramicrotome (Leica Ultracut S), were collected on copper grids and then stained with uranyl acetate and lead citrate. The sections were observed and photographed with a JEM-2000EXII transmission electron microscope.

Results

Association of Rab18 with Lysosomes in Neuronal Cells

In order to elucidate potential cellular roles of Rab18, we first examined subcellular distribution of Rab18 protein (Fig. 1). Using immunofluorescence staining, Rab18 appeared as vesicle-like puncta in cell soma and neurite-like processes in neuron-like PC12 cells differentiated by NGF treatment (Fig. 1a). To detect Rab18 in primary neurons, we stained Rab18 in cultured cortical neurons from wild-type and Rab18$^{-/-}$ mice [46]. In wild-type neurons, Rab18 again appeared as puncta structures throughout the cell body and neurites, whereas no immunoreactivity was found in Rab18$^{-/-}$ neurons (Fig. 1b), in which Rab18 protein expression was absent (Supplementary Fig. 1).

As an attempt to examine the identities of these Rab18-associated vesicles, we double stained PC12 cells with Rab18 antibody and markers for various organelles, including EGFP-Sec61β (endoplasmic reticulum (ER)), MitoTracker® (mitochondria), and early endosomes (EGFP-Rab5). We found that the majority of Rab18 protein was not colocalized with ER, mitochondria, or early endosomes (Fig. 1c). We next tested whether Rab18 can colocalize with lysosomes by applying the LysoTracker® probe to PC12 cells expressing EGFP-Rab18. Using colocalization analysis, we found that Rab18-associated vesicles is highly colocalized with lysosomes labeled with LysoTracker® in the cell body and neurites of NGF-differentiated PC12 cells (Fig. 1c).

Decreased Lysosomal Transport in Rab18$^{-/-}$ Neurons

Since we found that Rab18 was largely associated with lysosomes, which are actively transported along neurites in

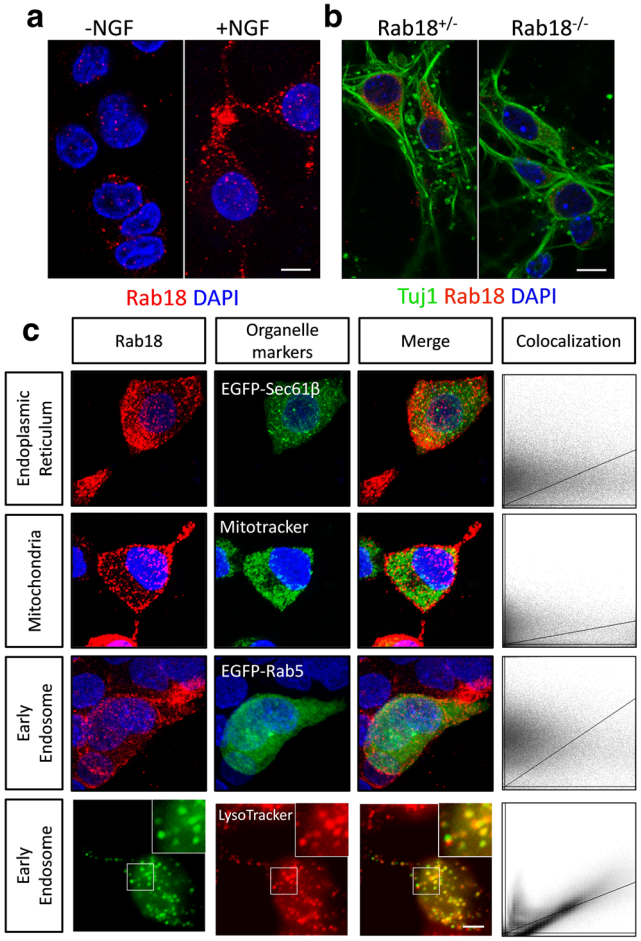

Fig. 1 Rab18 is localized to lysosomes in neurons. **a** Immunofluorescence staining of Rab18 (red) PC12 cells. Rab18 proteins exhibited punctate patterns and distributed at the cell soma and along neurites. **b** Immunofluorescence staining of Rab18 (red) and neuronal marker Tuj1 (green) in cultured neurons from wild-type and Rab18$^{-/-}$ mice. Rab18 appeared as punctates in cells. **c** Costaining of Rab18 (red) with various organelle markers. NGF-differentiated PC12 cells transfected with EGFP-Sec61β (ER) and EGFP-Rab5 (early endosome) plasmids or labeled by MitoTracker® (mitochondria) were immunostained by the Rab18 antibody. Rab18 was not colocalized with ER, mitochondria, and early endosomes in NGF-differentiated PC12 cells. Differentiated PC12 cells expressing EGFP-Rab18 (green) were labeled with LysoTracker® vital dye (red). Rab18 and lysosomes were largely colocalized (appears yellow). The inset showed a (3-fold) zoomed-in view of the box. Colocalization analysis was performed by plotting the fluorescent signal of GFP and RFP of each pixel within the cells (right panels). Fixed cells are counterstained with DAPI nuclear dye (blue). Scale bars 5 μm

neurons, we further investigated the dynamics of Rab18-associated vesicles in living cells. Cultured mouse cortical neurons and PC12 cells were transfected with EGFP-Rab18, and the dynamics of EGFP-Rab18-associated vesicles were recorded using time-lapse fluorescence microscopy. Indeed, we found that most Rab18-associated vesicles actively trafficked bi-directionally along the neurite in both primary neurons (Fig. 2a–c; Supplementary Video 1) and PC12 cells (Supplementary Fig. 2; Supplementary Video 2).

To test whether Rab18 plays a role in lysosomal transport, we monitored lysosomal movements in cultured *Rab18*$^{-/-}$ neurons (Fig. 2d–f). Cortical neurons were isolated from E16.5–18.5 *Rab18*$^{+/+}$ or *Rab18*$^{-/-}$ mouse embryos and cultured for 8–10 days in vitro (DIV). Lysosomes were then labeled with Lysotracker® and imaged by time-lapse fluorescence microscopy (Fig. 2d; Supplementary Videos 3 and 4). We found that the lysosomes in *Rab18*$^{-/-}$ cortical neurons moved at significantly slower rates in comparison with wild-type neurons (*Rab18*$^{-/-}$ 0.14 ± 0.03 μm/s vs. *Rab18*$^{+/+}$ 0.26 ± 0.04 μm/s, $n = 6$ fields from 3 individual cultures in each group, $p < 0.05$, Student's t test; Fig. 2e, f) while the lysosomal densities along neurites were comparable (*Rab18*$^{-/-}$ 0.20 ±

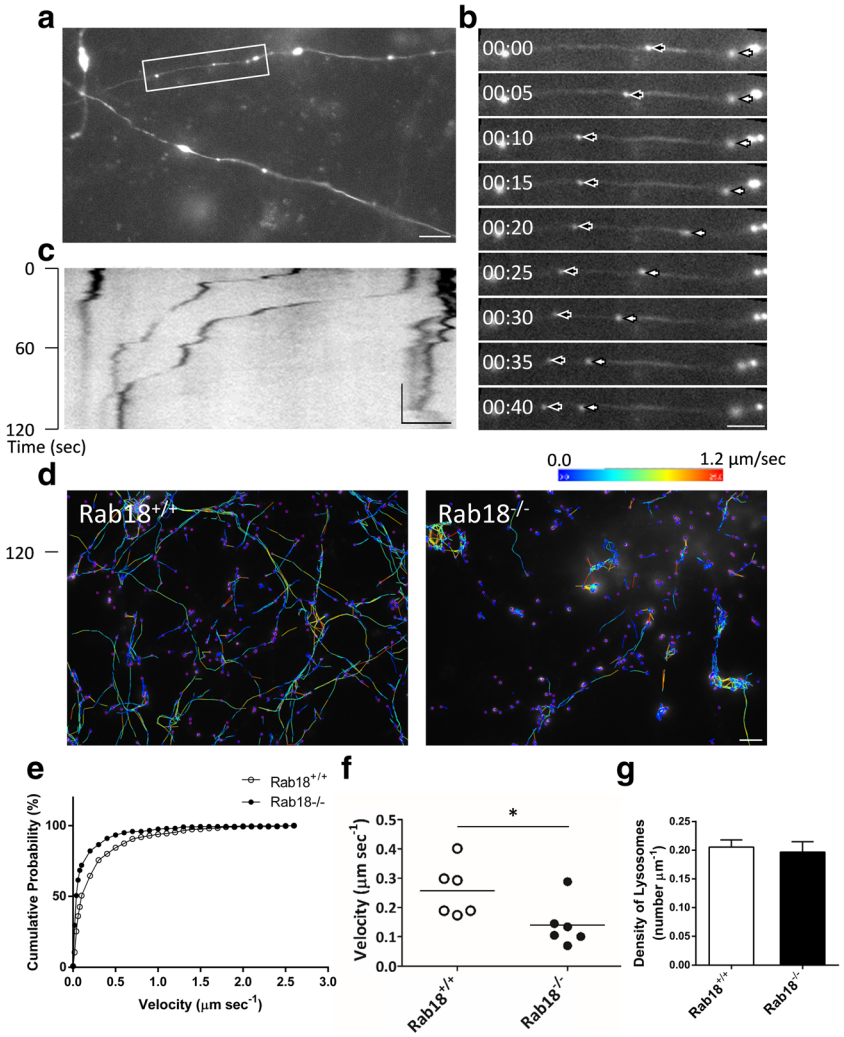

Fig. 2 Rab18 is involved in lysosomal trafficking. **a** Mouse cortical neurons expressing EGFP-Rab18. Rab18 was distributed in vesicle-like structures along the neurite. Scale bar 10 μm. The box indicated the region for **b** and **c**. **b** Time-lapse imaging of vesicle transport. Arrows indicated Rab18-associated vesicles moving along the neurite. Time was indicated in minute:second. Scale bar 5 μm. **c** The kymograph constructed from individual time-lapse images of the region in **b** through time. x-axis: distance and y-axis: time. Scale bars 5 μm and 30 s. **d** Lysosome transport in primary cortical neurons. Lysosomes were traced and plotted by TrackMate. The different color line corresponds to the instant velocity of each particles. Scale bar 10 μm. **e** The cumulative flow diagram demonstrated the cumulative distribution of lysosome velocities. The lysosomes in *Rab18*$^{-/-}$ cortical neurons had higher percentage in slow lysosomal transport region. **f** The average velocity of lysosomal transport in *Rab18*$^{-/-}$ cortical neurons is slower than that in *Rab18*$^{+/+}$ cells (n = 6 fields from three cultures). *$p < 0.05$, Student's t test. **g** Bar graph shows the density of lysosomes along neurites in Rab18$^{+/+}$ and Rab18$^{-/-}$ neurons. Error bars represent mean ± SEM; $n = 12$ neurites in each group

0.02 μm^{-1} vs. *Rab18*$^{+/+}$ 0.21 ± 0.01 μm^{-1}, $p = 0.70$, Student's *t* test, $n = 12$ in each group; Fig. 2g). These results implicated that Rab18 is important for lysosome transport in neurons.

Altered Autophagy Activities in Rab18-Defficient Neurons

The potential involvement of Rab18 in lysosomal functions urged us to examine signs of lysosomal dysfunction upon loss of *Rab18* in vivo. We used electron microscopy (EM) to image the CNS of *Rab18*$^{-/-}$ mouse in thin sections and found that, at 11 months of age, the dorsal root ganglion (DRG) exhibited an accumulation of electron-dense granules that assimilate the lipofuscin granules (Fig. 3a); the pigment granules composed of lipid-containing residues of lysosomal digestion [52, 53]. Previously, Rab18 has also been found to modulate macroautophagy in fibroblasts [44]; therefore, we next tested whether Rab18 plays a role in autophagy activities in the nervous system (Fig. 3b, c). We first used mouse neuronal culture infected with lentiviruses encoding two different Rab18 short hairpin RNA (shRNA) sequences, both of which effectively knocked down Rab18 expression by 80–90% (Supplementary Fig. 3). Autophagy activities were then examined by detecting the autophagy marker LC3 (microtubule-associated protein 1A/1B-light chain 3), which is recruited to autophagosomes in its cleaved form LC3-II. In cells expressing Rab18 shRNA, the level of LC3-II was increased by ~1.35-fold (shRab18-1981 1.38 ± 0.31, shRab18-7028 1.31 ± 0.34, $n = 3$; Fig. 3b). To verify this finding, the same experiment was performed in *Rab18*$^{-/-}$ neurons. We observed an even more dramatic increase in LC3-II in Rab18$^{-/-}$ neurons by ~2.3-fold (Rab18$^{-/-}$ 2.32 ± 0.54, $p < 0.05$, one-way ANOVA, followed by Fisher's least significant difference (LSD) test, $n = 3$; Fig. 3c). These results indicated an increase in autophagy activity and/or an accumulation of autophagosome, suggesting abnormal autophagy activities in Rab18-deficient neurons.

Molecular and Genetic Interactions Between Rab18 and Rab7

Previously, Rab7 was shown to associate with lysosomes and participate in lysosome biogenesis, trafficking, and autophagosome-lysosome fusion [54, 55]; therefore, we

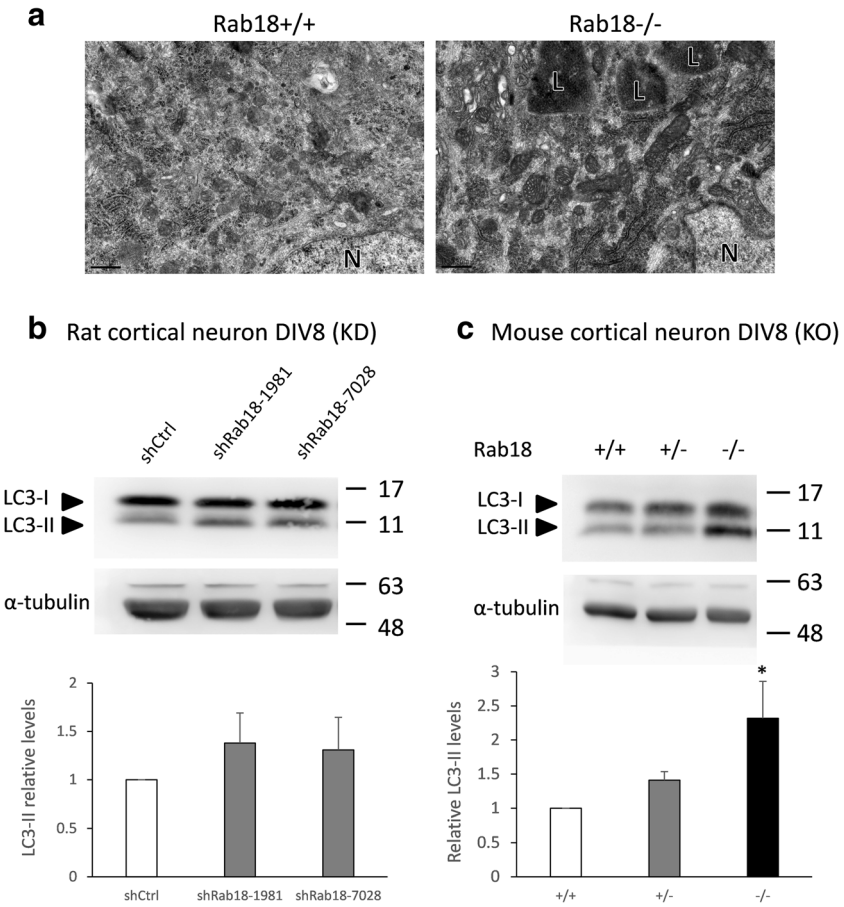

Fig. 3 Aberrant autophagy activities in Rab18 deficiency neurons. **a** Electron micrographs of DRG in *Rab18*$^{-/-}$ and wild-type mice. DRG neurons in *Rab18*$^{-/-}$ exhibited accumulations of lipofuscin, compared to wild-type littermates. L lipofuscin-like granules, N nucleus. Scale bar 0.5 μm. **b** Autophagy markers of LC3 levels in cortical neurons. Cultured cortical neurons were infected with lentivirus expressing Rab18 shRNA for 5 days from DIV 3. LC3-II protein level was analyzed by Western blotting. Bar graph shows increases of LC3-II level in Rab18-KD neurons. Error bar represent mean ± SEM; $n = 3$. **c** LC3-II levels in cultured cortical neurons from *Rab18*$^{-/-}$ and *Rab18*$^{+/-}$ mouse embryos and its littermates at DIV8. Bar graphs show increases in LC3-II level using Western blotting. Error bars represent mean ± SEM; *$p < 0.05$, one-way ANOVA, followed by Fisher's least significant difference (LSD) test. $n = 3$

postulated that Rab18 and Rab7 may have some connections in lysosomal functions. We first compared the distributions of Rab18 and Rab7 on lysosomes. Live primary cortical neurons coexpressing EGFP-Rab18 and mRFP-Rab7 were imaged by fluorescent microscopy. We found that most of Rab18-associated vesicles colocalized with Rab7 (Fig. 4a). Interestingly, using time-lapse recording, vesicles associated with both Rab18 and Rab7 were cotransported along neurites in primary neurons (Fig. 4b, c; Supplementary Video 5), implicating potential interactions between Rab18 and Rab7. Therefore, we performed coimmunoprecipitation (co-IP) in HEK293T cells cotransfected with EGFP-Rab18 and mRFP-Rab7. Proteins were extracted, precipitated by GFP-Trap®, and analyzed by western blot with Rab7 antibody (Fig. 4d). We found that Rab18 coprecipitated with Rab7, indicating molecular interaction between these two proteins. To verify the association of Rab18 with lysosomes and Rab7, lysosomes were isolated from adult mouse brain lysates. We found that both endogenous Rab18 and Rab7 were

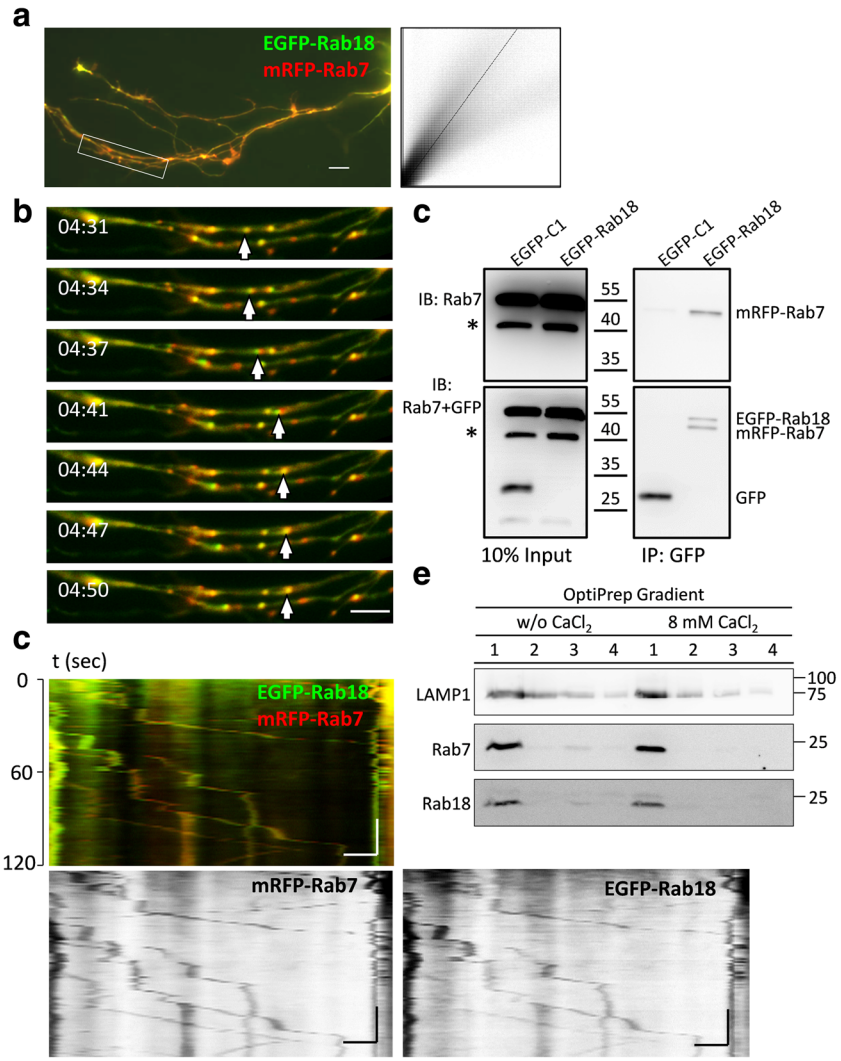

Fig. 4 Cotransportation and interaction of Rab18 and Rab7 in neurons. **a** EGFP-Rab18 and mRFP-Rab7 plasmids were cotransfected to eight to ten DIV primary cortical neurons. The box indicated the region of **b** and **c**. The right panel indicates colocalization analysis with GFP and RFP signals plotted for each pixel in the neurites. **b** Time-lapse imaging of EGFP-Rab18 and mRFP-Rab7 along neurites. Arrow indicated the colocalization of EGFP-Rab18 and mRFP-Rab7. Time was indicated in minute:second. **c** The kymograph constructed from individual time-lapse images of the region of **b** through time. *x*-axis: distance and *y*-axis: time. Scale bar 5 μm and 20 s. Bottom panels: Kymographs for each channel showed similar vesicle transport patterns. **d** EGFP-Rab18 and mRFP-Rab7 constructs were doubly transfected into HEK293T cells followed by immunoprecipitation (IP) using GFP-Trap® beads. Immunoblotting (IB) was performed for Rab7 (upper row) first and then probe for GFP (lower row). Rab7 was found to be in the EGFP-Rab18 IP lane, but not in the EGFP control IP lane. This result demonstrates an interaction between Rab18 and Rab7. Asterisk marks an unknown protein. **e** Rab18 and Rab7 were enriched in the lysosome fraction containing LAMP1. Lysosomes from 2-month-old mouse brain were separated by density gradient centrifugation (left) or further purification with $CaCl_2$ (right). Enriched lysosomes were mainly concentrated in fraction 1 marked by LAMP1

highly enriched in the vesicles with the lysosomal marker LAMP1 (Fig. 4e), further supporting the association of Rab18 with Rab7 on lysosomes.

To further explore possible functional relationship between these Rab18 and Rab7, we investigated Rab7 expression in cells deficient of Rab18. In cultured cortical neurons infected with lentivirus expressing Rab18 shRNA for 5 days, Rab7 expression was elevated by 1.6–1.8-fold (shRab18-1981 $1.63 \pm 0.12\%$, shRab18-7028 1.84 ± 0.21, $n = 5$; Fig. 5a). Similarly, in cortical neurons from *Rab18*$^{-/-}$ mouse brain, the expression of Rab7 had a ~1.5-fold increase compared to that in *Rab18*$^{+/+}$ neurons (1.55 ± 0.16, $n = 2$; Fig. 5b). These results suggested that the expression of Rab18 and Rab7 may be compensatory for lysosomal activities.

Discussion

In this study, we show that Rab18 localizes on vesicles actively traffic along the neurites in neuronal cells. We identify that many of these vesicles are lysosomes. The rates of lysosomal transport decrease in cultured neurons from *Rab18*$^{-/-}$ mice, suggesting an important role of Rab18 in lysosomal transport. Rab18 deficiency also causes aberrant lysosomal and autophagy activities in vivo and in vitro. Interestingly, Rab18 colocalizes and cofractionates with Rab7 on lysosomes, and coprecipitates with Rab7 in vitro. Expression of Rab7 is elevated in Rab18 knockdown and knockout neurons, implicating a compensatory effect. Altogether, these findings suggest that Rab18 and Rab7 proteins may cooperate in lysosome functions and autophagy in neurons. These results also provide new insights into the etiology of WARBM and a potential link between WARBM and CMT neuropathy.

Potential Roles of Rab18 in Lysosomal Transport and Autophagy

Our new finding that Rab18 is involved in lysosomal transport and autophagy could be an important mechanism of WARBM pathogenesis. Lysosome plays an essential role in the degradation of damaged organelles, misfolded proteins, and protein aggregates. Impaired lysosomal functions and autophagy may result in accumulation of neurotoxic proteins. These abnormally accumulated proteins in the neurites may be implicated in late-onset neurodegenerative diseases, such as Alzheimer's disease, Parkinson's disease, amyotrophic lateral sclerosis (ALS), and some types of lysosomal storage diseases [56–60]. These late-onset axonal degenerative diseases present many common characteristics: progressive pathology, functional declines with age, and distal axonal degeneration followed by neuronal loss [57], all of which were observed in our *Rab18*$^{-/-}$ mice and WARBM patients.

Supporting our findings, several studies also reported potential functions of Rab18 on lysosomal activities. Previously, Rab18 has been found to colocalize with autophagosomes and lysosomes in human breast adenocarcinoma cell line MCF-7 treated with nanoparticles [61]. A recent study also showed an association of Rab18 with lysosomes and Rab7 in the developing cortical neurons [62]. In utero electroporation of Rab18 shRNA showed defects in neuronal migration, possibly due to a dysregulation of N-cadherin degradation by lysosomal pathway. More recently, RAB18 has been identified as a positive regulator for macroautophagy and proteostasis in primary human fibroblasts [44]. RAB18 knockdown by shRNA resulted in a decreased autophagic activity, while its overexpression enhances the degradative pathway. These results are consistent with the involvement of lysosomal dysfunctions in the pathogenesis of WARBM.

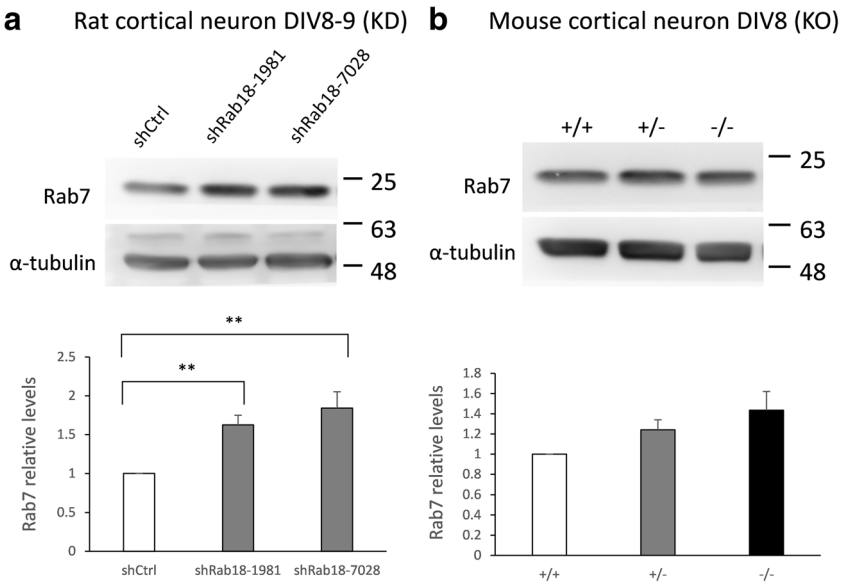

Fig. 5 Increase in Rab7 expression in Rab18-deficient neurons. **a** Rab7 protein expression was significantly elevated in the Rab18 knockdown neurons (shRab18-1981 and shRab18-7028) compared to shCtrl. Error bars represent SEM; $n = 5$. $^{**}p < 0.01$, one-way ANOVA, followed by Fisher's least significant difference (LSD) test. **b** Rab7 protein expression was gradually elevated in Rab18$^{+/-}$ and Rab18$^{-/-}$ neurons compared to wild-type neuron. Error bars represent SEM; $n = 2$

Possible Common Causes Between WARBM and CMT2B

Perhaps one of the most surprising findings in the current study is that Rab18 is linked to Rab7 molecularly and genetically. Rab7 is involved in membrane trafficking from early endosomes to late endosomes and lysosomes [11, 54]. Recently, Rab7 has also been shown to be essential for the fusion of autophagosomes with lysosomes [55]. In the current study, Rab18 deficiency leads to an increase in Rab7 expression in the murine neurons. Although the mechanism remains elusive, it is likely to be a compensatory effect, further supporting their collaborative role in lysosomal functions.

Interestingly, mutations in human *RAB7* result in CMT2B, a type of sensory neuropathy caused by impaired retrograde transport. In the *Rab18*$^{-/-}$ mice, we observed signs of sensory axonal degeneration in the gracile fasciculus of the spinal cord and dorsal roots of lumbar spinal nerves [46]. These pathological findings could be the major cause of progressive visual loss and progressive limb spasticity in WARBM patients. The phenotypic similarities between *Rab18* and *Rab7* mutations strongly suggest that Rab18 and Rab7 may share related functions in the lysosomal/autophagy pathway. Thus lysosomal accumulation and defects in autophagy may be common pathways that contribute to the neuropathic phenotypes in both WARBM and CMT. Consistent with this idea, an autosomal recessive disease of Black Russian Terriers, previously described as a juvenile-onset, laryngeal paralysis and polyneuropathy similar to CMT in humans [63], has been found to result from a homozygous mutation of *RAB3GAP1*, a causative gene for human WARBM [64]. These dogs exhibited phenotypes of human CMT and WARBM patients, suggesting that these two disease share many common phenotypes and causes.

In summary, Rab18 dysfunction results in abnormal lysosomal trafficking and autophagy activities in neurons, potentially leading to axonal degeneration in WARBM. The genetic and molecular interactions between Rab18 and Rab7 suggested that WARBM and CMT may share overlapping mechanisms during disease progression.

Acknowledgements We appreciate Dr. Mu-Ming Poo (University of California, Berkeley), Dr. Chih-Chiang Chan (National Taiwan University), and Ms. Elise Shen (University of Texas, Austin) for helpful comments and suggestions. The authors also wish to thank the Instrumentation Resource Center, National Yang-Ming University, and the National RNAi Core Facility at Academia Sinica, Taiwan for their technical support.

Authors' Contributions Study conception and design: JWT, CJH, LSK, MJF, and CYT. Project supervision: JWT. Data collection: FSN, LLL, CYC, PCW, YTL, BSR, and CYT. Data analysis and interpretation: FSN, LLL, JWT, MJF, and LSK. Drafting the article: FSN and JWT. Final approval of the version to be published: all authors.

Funding This work was supported by the grants of Yen Tjing Ling Medical Foundation (CI-103-4), the Ministry of Science and Technology (NSC 101-2320-B-010-077-MY2, 102-2314-B-075-079, 103-2628-B-010-002-MY3, 104-2633-H-010-001, 104-2745-B-075-001, 105-2633-B-009-003, 106-2321-B-075-001, 106-2628-B-010-002-MY3, and 107-2321-B-075-001), Taipei Veterans General Hospital-University System of Taiwan (VGHUST106-G7-5-2), National Health Research Institutes (NHRI-EX103-10314NC), and Academia Sinica, Taiwan (AS-104-TP-B09 and 2396-105-0100) to JWT; and Taiwan National Science Council (NSC 102-2314-B-075-005-MY3), Taipei Veterans General Hospital (V103E9-004 and V102C-173), and the Ministry of Education Taiwan, Aim for the Top University Plan to CJH. This work is also supported by the Development and Construction Program of NYMU School of Medicine (107F-M01-0502) and the Brain Research Center, NYMU through the Featured Areas Research Center Program within the framework of the Higher Education Sprout Project by the Ministry of Education (MOE), Taiwan.

Availability of Supporting Data The datasets used and/or analyzed during the current study are available from the corresponding author on reasonable request.

Compliance with Ethical Standards

Ethical Approval and Consent to Participate Not applicable.

Consent for Publication Not applicable.

Competing Interests The authors declare that they have no competing interests.

Publisher's Note Springer Nature remains neutral with regard to jurisdictional claims in published maps and institutional affiliations.

References

1. Warburg M, Sjo O, Fledelius HC, Pedersen SA (1993) Autosomal recessive microcephaly, microcornea, congenital cataract, mental retardation, optic atrophy, and hypogenitalism. Micro syndrome. Am J Dis Child 147(12):1309–1312
2. Megarbane A, Choueiri R, Bleik J, Mezzina M, Caillaud C (1999) Microcephaly, microphthalmia, congenital cataract, optic atrophy, short stature, hypotonia, severe psychomotor retardation, and cerebral malformations: a second family with micro syndrome or a new syndrome? J Med Genet 36(8):637–640
3. Ainsworth JR, Morton JE, Good P, Woods CG, George ND, Shield JP, Bradbury J, Henderson MJ et al (2001) Micro syndrome in Muslim Pakistan children. Ophthalmology 108(3):491–497
4. Graham JM Jr, Hennekam R, Dobyns WB, Roeder E, Busch D (2004) MICRO syndrome: an entity distinct from COFS syndrome. Am J Med Genet A 128a(3):235–245. https://doi.org/10.1002/ajmg.a.30060
5. Rodriguez Criado G, Rufo M, Gomez de Terreros I (1999) A second family with micro syndrome. Clin Dysmorphol 8(4):241–245
6. Bem D, Yoshimura S, Nunes-Bastos R, Bond FC, Kurian MA, Rahman F, Handley MT, Hadzhiev Y et al (2011) Loss-of-function mutations in RAB18 cause Warburg micro syndrome. Am J Hum Genet 88(4):499–507. https://doi.org/10.1016/j.ajhg.2011.03.012
7. Handley MT, Aligianis IA (2012) RAB3GAP1, RAB3GAP2 and RAB18: disease genes in micro and Martsolf syndromes. Biochem Soc Trans 40(6):1394–1397. https://doi.org/10.1042/bst20120169

8. Handley MT, Morris-Rosendahl DJ, Brown S, Macdonald F, Hardy C, Bem D, Carpanini SM, Borck G et al (2013) Mutation spectrum in RAB3GAP1, RAB3GAP2, and RAB18 and genotype-phenotype correlations in Warburg micro syndrome and Martsolf syndrome. Hum Mutat 34(5):686–696. https://doi.org/10.1002/humu.22296
9. Liegel RP, Handley MT, Ronchetti A, Brown S, Langemeyer L, Linford A, Chang B, Morris-Rosendahl DJ, Carpanini S, Posmyk R, Harthill V, Sheridan E, Abdel-Salam GMH, Terhal PA, Faravelli F, Accorsi P, Giordano L, Pinelli L, Hartmann B, Ebert AD, Barr FA, Aligianis IA, Sidjanin DJ (2013) Loss-of-function mutations in TBC1D20 cause cataracts and male infertility in blind sterile mice and Warburg micro syndrome in humans. Am J hum genet doi: https://doi.org/10.1016/j.ajhg.2013.10.011, 93, 1001, 1014
10. Hutagalung AH, Novick PJ (2011) Role of Rab GTPases in membrane traffic and cell physiology. Physiol Rev 91(1):119–149. https://doi.org/10.1152/physrev.00059.2009
11. Bucci C, De Luca M (2012) Molecular basis of Charcot-Marie-Tooth type 2B disease. Biochem Soc Trans 40(6):1368–1372. https://doi.org/10.1042/BST20120197
12. Cogli L, Piro F, Bucci C (2009) Rab7 and the CMT2B disease. Biochem Soc Trans 37 (Pt 5):1027–1031. doi:https://doi.org/10.1042/bst0371027
13. Hidestrand P, Vasconez H, Cottrill C (2009) Carpenter syndrome. J Craniofac Surg 20(1):254–256. https://doi.org/10.1097/SCS.0b013e318184357a
14. Eggenschwiler JT, Espinoza E, Anderson KV (2001) Rab23 is an essential negative regulator of the mouse Sonic hedgehog signalling pathway. Nature 412(6843):194–198. https://doi.org/10.1038/35084089
15. Jenkins D, Seelow D, Jehee FS, Perlyn CA, Alonso LG, Bueno DF, Donnai D, Josifova D et al (2007) RAB23 mutations in Carpenter syndrome imply an unexpected role for hedgehog signaling in cranial-suture development and obesity. Am J Hum Genet 80(6):1162–1170. https://doi.org/10.1086/518047
16. Hurvitz H, Gillis R, Klaus S, Klar A, Gross-Kieselstein F, Okon E (1993) A kindred with Griscelli disease: spectrum of neurological involvement. Eur J Pediatr 152(5):402–405
17. Haraldsson A, Weemaes CM, Bakkeren JA, Happle R (1991) Griscelli disease with cerebral involvement. Eur J Pediatr 150(6):419–422
18. Anikster Y, Huizing M, Anderson PD, Fitzpatrick DL, Klar A, Gross-Kieselstein E, Berkun Y, Shazberg G et al (2002) Evidence that Griscelli syndrome with neurological involvement is caused by mutations in RAB27A, not MYO5A. Am J Hum Genet 71(2):407–414. https://doi.org/10.1086/341606
19. Lu IL, Chen C, Tung CY, Chen HH, Pan JP, Chang CH, Cheng JS, Chen YA et al (2018) Identification of genes associated with cortical malformation using a transposon-mediated somatic mutagenesis screen in mice. Nat Commun 9(1):2498. https://doi.org/10.1038/s41467-018-04880-8
20. Seixas E, Barros M, Seabra MC, Barral DC (2013) Rab and Arf proteins in genetic diseases. Traffic 14(8):871–885. https://doi.org/10.1111/tra.12072
21. Giannandrea M, Bianchi V, Mignogna ML, Sirri A, Carrabino S, D'Elia E, Vecellio M, Russo S et al (2010) Mutations in the small GTPase gene RAB39B are responsible for X-linked mental retardation associated with autism, epilepsy, and macrocephaly. Am J Hum Genet 86(2):185–195. https://doi.org/10.1016/j.ajhg.2010.01.011
22. Lutcke A, Parton RG, Murphy C, Olkkonen VM, Dupree P, Valencia A, Simons K, Zerial M (1994) Cloning and subcellular localization of novel rab proteins reveals polarized and cell type-specific expression. J Cell Sci 107(Pt 12):3437–3448
23. Yu H, Leaf DS, Moore HP (1993) Gene cloning and characterization of a GTP-binding Rab protein from mouse pituitary AtT-20 cells. Gene 132(2):273–278
24. Martin S, Driessen K, Nixon SJ, Zerial M, Parton RG (2005) Regulated localization of Rab18 to lipid droplets: effects of lipolytic stimulation and inhibition of lipid droplet catabolism. J Biol Chem 280(51):42325–42335. https://doi.org/10.1074/jbc.M506651200
25. Ozeki S, Cheng J, Tauchi-Sato K, Hatano N, Taniguchi H, Fujimoto T (2005) Rab18 localizes to lipid droplets and induces their close apposition to the endoplasmic reticulum-derived membrane. J Cell Sci 118(Pt 12):2601–2611. https://doi.org/10.1242/jcs.02401
26. Martin S, Parton RG (2008) Characterization of Rab18, a lipid droplet-associated small GTPase. Methods Enzymol 438:109–129. https://doi.org/10.1016/S0076-6879(07)38008-7
27. Pulido MR, Diaz-Ruiz A, Jimenez-Gomez Y, Garcia-Navarro S, Gracia-Navarro F, Tinahones F, Lopez-Miranda J, Fruhbeck G et al (2011) Rab18 dynamics in adipocytes in relation to lipogenesis, lipolysis and obesity. PLoS One 6(7):e22931. https://doi.org/10.1371/journal.pone.0022931
28. Pulido MR, Rabanal-Ruiz Y, Almabouada F, Diaz-Ruiz A, Burrell MA, Vazquez MJ, Castano JP, Kineman RD et al (2013) Nutritional, hormonal, and depot-dependent regulation of the expression of the small GTPase Rab18 in rodent adipose tissue. J Mol Endocrinol 50(1):19–29. https://doi.org/10.1530/JME-12-0140
29. Brasaemle DL, Dolios G, Shapiro L, Wang R (2004) Proteomic analysis of proteins associated with lipid droplets of basal and lipolytically stimulated 3T3-L1 adipocytes. J Biol Chem 279(45):46835–46842. https://doi.org/10.1074/jbc.M409340200
30. Makino A, Hullin-Matsuda F, Murate M, Abe M, Tomishige N, Fukuda M, Yamashita S, Fujimoto T et al (2016) Acute accumulation of free cholesterol induces the degradation of perilipin 2 and Rab18-dependent fusion of ER and lipid droplets in cultured human hepatocytes. Mol Biol Cell 27(21):3293–3304. https://doi.org/10.1091/mbc.E15-10-0730
31. Li C, Luo X, Zhao S, Siu GK, Liang Y, Chan HC, Satoh A, Yu SS (2017) COPI-TRAPPII activates Rab18 and regulates its lipid droplet association. EMBO J 36(4):441–457. https://doi.org/10.15252/embj.201694866
32. Dubiel D, Bintig W, Kahne T, Dubiel W, Naumann M (2017) Cul3 neddylation is crucial for gradual lipid droplet formation during adipogenesis. Biochim Biophys Acta 1864(8):1405–1412. https://doi.org/10.1016/j.bbamcr.2017.05.009
33. Gerondopoulos A, Bastos RN, Yoshimura S, Anderson R, Carpanini S, Aligianis I, Handley MT, Barr FA (2014) Rab18 and a Rab18 GEF complex are required for normal ER structure. J Cell Biol 205(5):707–720. https://doi.org/10.1083/jcb.201403026
34. Dejgaard SY, Murshid A, Erman A, Kizilay O, Verbich D, Lodge R, Dejgaard K, Ly-Hartig TB et al (2008) Rab18 and Rab43 have key roles in ER-Golgi trafficking. J Cell Sci 121(Pt 16):2768–2781. https://doi.org/10.1242/jcs.021808
35. Handley MT, Carpanini SM, Mali GR, Sidjanin DJ, Aligianis IA, Jackson IJ, FitzPatrick DR (2015) Warburg micro syndrome is caused by RAB18 deficiency or dysregulation. Open Biol 5(6):150047. https://doi.org/10.1098/rsob.150047
36. Gillingham AK, Sinka R, Torres IL, Lilley KS, Munro S (2014) Toward a comprehensive map of the effectors of rab GTPases. Dev Cell 31(3):358–373. https://doi.org/10.1016/j.devcel.2014.10.007
37. Malagon MM, Cruz D, Vazquez-Martinez R, Peinado JR, Anouar Y, Tonon MC, Vaudry H, Gracia-Navarro F et al (2005) Analysis of Rab18 and a new golgin in the secretory pathway. Ann N Y Acad Sci 1040:137–139. https://doi.org/10.1196/annals.1327.017
38. Vazquez-Martinez R, Cruz-Garcia D, Duran-Prado M, Peinado JR, Castano JP, Malagon MM (2007) Rab18 inhibits secretory activity in neuroendocrine cells by interacting with secretory granules. Traffic 8(7):867–882. https://doi.org/10.1111/j.1600-0854.2007.00570.x

39. Salloum S, Wang H, Ferguson C, Parton RG, Tai AW (2013) Rab18 binds to hepatitis C virus NS5A and promotes interaction between sites of viral replication and lipid droplets. PLoS Pathog 9(8): e1003513. https://doi.org/10.1371/journal.ppat.1003513
40. Tang WC, Lin RJ, Liao CL, Lin YL (2014) Rab18 facilitates dengue virus infection by targeting fatty acid synthase to sites of viral replication. J Virol 88(12):6793–6804. https://doi.org/10.1128/jvi.00045-14
41. Chan SC, Lo SY, Liou JW, Lin MC, Syu CL, Lai MJ, Chen YC, Li HC (2011) Visualization of the structures of the hepatitis C virus replication complex. Biochem Biophys Res Commun 404(1):574–578. https://doi.org/10.1016/j.bbrc.2010.12.037
42. Hashim S, Mukherjee K, Raje M, Basu SK, Mukhopadhyay A (2000) Live Salmonella modulate expression of Rab proteins to persist in a specialized compartment and escape transport to lysosomes. J Biol Chem 275(21):16281–16288
43. Dansako H, Hiramoto H, Ikeda M, Wakita T, Kato N (2014) Rab18 is required for viral assembly of hepatitis C virus through trafficking of the core protein to lipid droplets. Virology 462-463:166–174. https://doi.org/10.1016/j.virol.2014.05.017
44. Feldmann A, Bekbulat F, Huesmann H, Ulbrich S, Tatzelt J, Behl C, Kern A (2017) The RAB GTPase RAB18 modulates macroautophagy and proteostasis. Biochem Biophys Res Commun 486(3):738–743. https://doi.org/10.1016/j.bbrc.2017.03.112
45. Carpanini SM, McKie L, Thomson D, Wright AK, Gordon SL, Roche SL, Handley MT, Morrison H et al (2014) A novel mouse model of Warburg micro syndrome reveals roles for RAB18 in eye development and organisation of the neuronal cytoskeleton. Dis Model Mech 7(6):711–722. https://doi.org/10.1242/dmm.015222
46. Cheng CY, Wu JC, Tsai JW, Nian FS, Wu PC, Kao LS, Fann MJ, Tsai SJ et al (2015) ENU mutagenesis identifies mice modeling Warburg micro syndrome with sensory axon degeneration caused by a deletion in Rab18. Exp Neurol 267:143–151. https://doi.org/10.1016/j.expneurol.2015.03.003
47. Tai CY, Mysore SP, Chiu C, Schuman EM (2007) Activity-regulated N-cadherin endocytosis. Neuron 54(5):771–785. https://doi.org/10.1016/j.neuron.2007.05.013
48. Liu YT, Nian FS, Chou WJ, Tai CY, Kwan SY, Chen C, Kuo PW, Lin PH et al (2016) PRRT2 mutations lead to neuronal dysfunction and neurodevelopmental defects. Oncotarget 7(26):39184–39196. https://doi.org/10.18632/oncotarget.9258
49. Jheng GW, Hur SS, Chang CM, Wu CC, Cheng JS, Lee HH, Chung BC, Wang YK et al (2018) Lis1 dysfunction leads to traction force reduction and cytoskeletal disorganization during cell migration. Biochem Biophys Res Commun 497(3):869–875. https://doi.org/10.1016/j.bbrc.2018.02.151
50. Chen JL, Chang CH, Tsai JW (2018) Gli2 rescues delays in brain development induced by Kif3a dysfunction. Cereb Cortex 29:751–764. https://doi.org/10.1093/cercor/bhx356
51. Dunn KW, Kamocka MM, McDonald JH (2011) A practical guide to evaluating colocalization in biological microscopy. Am J Physiol Cell Physiol 300(4):C723–C742. https://doi.org/10.1152/ajpcell.00462.2010
52. Mitsumori K, Maita K, Shirasu Y (1981) An ultrastructural study of spinal nerve roots and dorsal root ganglia in aging rats with spontaneous radiculoneuropathy. Vet Pathol 18(6):714–726. https://doi.org/10.1177/030098588101800602
53. Samorajski T, Ordy JM, Rady-Reimer P (1968) Lipofuscin pigment accumulation in the nervous system of aging mice. Anat Rec 160(3):555–574. https://doi.org/10.1002/ar.1091600305
54. Bucci C, Thomsen P, Nicoziani P, McCarthy J, van Deurs B (2000) Rab7: a key to lysosome biogenesis. Mol Biol Cell 11(2):467–480
55. Hyttinen JM, Niittykoski M, Salminen A, Kaarniranta K (2013) Maturation of autophagosomes and endosomes: a key role for Rab7. Biochim Biophys Acta 1833(3):503–510. https://doi.org/10.1016/j.bbamcr.2012.11.018
56. Millecamps S, Julien JP (2013) Axonal transport deficits and neurodegenerative diseases. Nat Rev Neurosci 14(3):161–176. https://doi.org/10.1038/nrn3380
57. Morfini GA, Burns M, Binder LI, Kanaan NM, LaPointe N, Bosco DA, Brown RH Jr, Brown H et al (2009) Axonal transport defects in neurodegenerative diseases. J Neurosci 29(41):12776–12786. https://doi.org/10.1523/jneurosci.3463-09.2009
58. Nelson MP, Tse TE, O'Quinn DB, Percival SM, Jaimes EA, Warnock DG, Shacka JJ (2014) Autophagy-lysosome pathway associated neuropathology and axonal degeneration in the brains of alpha-galactosidase A-deficient mice. Acta Neuropathol Commun 2(1):20. https://doi.org/10.1186/2051-5960-2-20
59. Nixon RA (2013) The role of autophagy in neurodegenerative disease. Nat Med 19(8):983–997. https://doi.org/10.1038/nm.3232
60. Zhang L, Sheng R, Qin Z (2009) The lysosome and neurodegenerative diseases. Acta Biochim Biophys Sin Shanghai 41(6):437–445
61. Li JK, Fei P, Li Y, Huang QJ, Zhang Q, Zhang X, Rao YQ, Li J et al (2016) Identification of novel KIF11 mutations in patients with familial exudative vitreoretinopathy and a phenotypic analysis. Sci Rep 6:26564. https://doi.org/10.1038/srep26564
62. Wu Q, Sun X, Yue W, Lu T, Ruan Y, Chen T, Zhang D (2016) RAB18, a protein associated with Warburg micro syndrome, controls neuronal migration in the developing cerebral cortex. Mol Brain 9:19. https://doi.org/10.1186/s13041-016-0198-2
63. Granger N (2011) Canine inherited motor and sensory neuropathies: an updated classification in 22 breeds and comparison to Charcot-Marie-tooth disease. Vet J 188(3):274–285. https://doi.org/10.1016/j.tvjl.2010.06.003
64. Mhlanga-Mutangadura T, Johnson GS, Schnabel RD, Taylor JF, Johnson GC, Katz ML, Shelton GD, Lever TE et al (2016) A mutation in the Warburg syndrome gene, RAB3GAP1, causes a similar syndrome with polyneuropathy and neuronal vacuolation in black Russian terrier dogs. Neurobiol Dis 86:75–85. https://doi.org/10.1016/j.nbd.2015.11.016